Indian J. pure appl. Math., **31**(10) : 1339-1351, October 2000

PROBABILITY DENSITY FUNCTION APPROACH TO NON-PREMIXED TURBULENT FLAMES

V. RAMANUJACHARI AND S. BALAKRISHNA

Institute of Armament Technology, Pune 411 025, *India*

AND

S. GANESAN

Gas Turbine Research Establishment, Bangalore 560 093, *India*

(*Received* 22 *March* 1999; *after revision* 30 *December* 1999; *accepted* 22 *February* 2000)

The turbulent non-premixed flames are of interest in practical applications such as jet engines, diesel engines, steam boilers and furnaces. The understanding of non-premixed flames is obtained by flow computation based on mathematical models. The flow field of a non-premixed turbulent flame has been modelled using the steady conservation equations of mass, axial momentum, mean mixture fraction, turbulent kinetic energy, turbulent energy dissipation rate and square of mixture fraction fluctuations in axisymmetric coordinates. The computations of state relationships involve conventional adiabatic mixing calculations, with the local state of the mixture specified by the mixture fraction, f, the fraction of the material at a point which originated at the injector. Consistent with the assumption of equal exchange coefficients, the instantaneous properties may be treated as a function only of mixture fraction. This facilitates the determination of all scalar properties (temperature, composition and density), as a function of mixture fraction. Mean scalar properties such as density and temperature are computed using various probability density functions based on periodic and non-periodic random distributions. The case study considered for validation is a combusting propane gas jet. The predictions show that the maximum mean temperatures are reached away from the axis of the jet. All these temperatures are below the adiabatic flame temperature for stoichiometric combustion (2270K). These lower values are due to turbulent "unmixedness", which is represented in the calculations by the rectangular, triangular, clipped-Gaussian and beta distributions. The temperature distributions are predicted reasonably well throughout the flow region by both clipped-Gaussian and beta distributions, whereas, the rectangular and triangular distributions predicted well the near centerline regions of the jet indicating their limitation to compute the flow at the edges of the jet flame.

Key Words : Probability Density Function; Turbulence; Combustion; Gaussian Distribution; Beta Distribution

NOMENCLATURE

a - **Acceleration due to gravity**

$C_{\varepsilon_1}\ C_{\varepsilon_2}\ C_{g_1}\ C_{g_2}\ C_\mu$ - **Turbulence constants**

d - **Exit diameter**

f - **Mixture fraction**

g - **Square of mixture fraction fluctuations**

$H(x)$ - Heaviside function of x

k - Turbulent Kinetic energy

N - Total number of steps

$P(\phi)$ - Probability density function of any ϕ

r - Radial coordinate

S_ϕ - Source term of any ϕ

SC - Schmidt number

$\bar{u}, \bar{v}$ - Velocity components

x - Axial distance; any dummy variable

Greek Letters

α, β - Beta function parameters

$\delta(x)$ - Dirac-delta function of x

ε - Dissipation rate

ϕ - General dependent variable

μ - Dynamic viscosity

ρ - Density

σ_ϕ - Turbulent Prandtl/Schmidt number

Subscript

° - Nozzle exit condition

t - Turbulent quantity

∞ - Ambient value

$-$ - Time averaged quantity

$'$ - Fluctuating quantity

INTRODUCTION

The turbulent non-premixed flames are of interest in practical applications such as jet engines, diesel engines, steam boilers and furnaces. The understanding of non-premixed flames is obtained by flow computation based on LHF model, which assumes that the chemicals react to equilibrium as fast as they mix. The formulations of the LHF models in the past[1 & 2] employed the Reynolds-averaged form of the governing equations. Favre-averaged form of the equations with the effect of gravity on turbulence was employed and validated with the experiments of Mao *et al.*[1] by Ramanujachari and Natarajan[3]. Certain characteristics of turbulent non-premixed flames such as scalar dissipation rate are computed and reported by Ganesan and Ramanujachari[4]. Ganesan *et al.*[5] evaluated the scalars using beta probability density function and gave an account of the mathematical complexities involved in the methodology of computation of mean-temperature. The objective of the present study is to perform additional computations, using various probability density functions based on periodic and non-periodic random distributions to bring out the characteristics of non-premixed flames in addition to the validation of theoretical results with the experimental data of Mao *et al.*[1]

GOVERNING EQUATIONS OF LHF MODEL

The basic premise of the LHF model is that the inter-phase transport rates are fast in comparison to the rate of development of the flow as a whole. This implies that all phases have the same velocity and temperature at each point in the flow. The Reynolds-averaged governing equations for the LHF model, based on the boundary layer assumptions, are written as follows :

$$(\partial/\partial x)(\overline{\rho}\,\overline{u}\,\overline{\phi}) + (1/r)(\partial/\partial r)(r\,\overline{\rho}\,\overline{v}\,\overline{\phi}) = (1/r)(\partial/\partial r)(r\mu_{eff,\phi}(\partial/\partial r)\,\overline{\phi}) + S_{\phi}. \quad \ldots (1)$$

The conservation equations of mass ($\overline{\phi} = 1$), momentum, mixture fraction, turbulent kinetic energy, rate of dissipation of turbulent kinetic energy and the square of the mixture fraction fluctuations are obtained using eq. 1, and the expressions for $\overline{\phi}$, $\mu_{eff,\phi}$ and S_{ϕ} are shown in Table I along with the appropriate empirical constants.

STATE RELATIONSHIPS

The computations of state relationships involve conventional adiabatic mixing calculations, with the local state of the mixture specified by the mixture fraction, f, the fraction of the material at a point which originated at the injector. Turbulent mixing of the conserved scalar such as mixture fraction f is an unsolved problem. Finding methods of predicting the conserved scalar mixing has been, and continues to be, the major topic of research. Consistent with the assumption of equal exchange coefficients, the instantaneous properties may be treated as a function only of mixture fraction. This facilitates the determination of all scalar properties (temperature, composition and density), as a function of mixture fraction. The time-averaged mean and variance of the flow properties are then found from the probability density function for mixture fraction, $P(f)$, as follows :

$$\overline{\phi} = \int_0^1 \phi(f)\,P(f)df \quad \ldots (2)$$

and

$$\overline{\phi'^2} = \int_0^1 [\phi(f) - \overline{\phi}]^2\,P(f)\,df. \quad \ldots (3)$$

In eqs. (2) and (3), $\phi(f)$ is known from the state relationships. A functional form must be assumed for $P(f)$. The fundamental forms can be based on both periodic and non-periodic random functions. The functions used are rectangular, triangular, clipped-Gaussian and beta distributions and are discussed below :

Rectangular Distribution

$$P(f) = 0.5\,[\delta(f - f_{-}) + \delta(f - f_{+})], \quad \ldots (4)$$

where

$$f_{+} = \overline{f} + \sqrt{g}\,; f_{-} = \overline{f} - \sqrt{g}.$$

Triangular Distribution

$$P(f) = \frac{1}{2\sqrt{3g}}\,[H(f - f_{-}) - H(f - f_{+})], \quad \ldots (5)$$

where

$$f_+ = \bar{f} + \sqrt{3g}; f_- = \bar{f} - \sqrt{3g}.$$

Clipped Gaussian Distribution

$$P(f) = \frac{1}{\sigma\sqrt{2\pi}} e^{-1/2\left(\frac{f-\mu}{\sigma}\right)^2} + A\,\delta(0) + B\,\delta(1), \quad \ldots (6)$$

where

$$A = \frac{1}{\sigma\sqrt{2\pi}} \int_{-\infty}^{0} e^{-1/2\left(\frac{f-\mu}{\sigma}\right)^2} df$$

and

$$B = \frac{1}{\sigma\sqrt{2\pi}} \int_{1}^{\infty} e^{-1/2\left(\frac{f-\mu}{\sigma}\right)^2} df.$$

The parameters of clipped-Gaussian distribution, μ and σ are calculated by solving the equations given below :

$$\bar{f} = \int_0^1 f P(f) df \quad \ldots (7)$$

and

$$g = \int_0^1 (f-\bar{f})^2 P(f)\, df. \quad \ldots (8)$$

Beta Distribution

$$P(f) = f^{\alpha-1}(1-f)^{\beta-1} / \int_0^1 f^{\alpha-1}(1-f)^{\beta-1} df, \quad \ldots (9)$$

where

$$\alpha = \bar{f}[\bar{f}(1-\bar{f})/g - 1]$$

and

$$\beta = (1-\bar{f})[\bar{f}(1-\bar{f})/g - 1]$$

with the condition $g \leq \bar{f}(1-\bar{f})$.

Both $\bar{f}$ and g are computed from the solution of governing equations. The time-averaged values of density, temperature and species mass fractions are obtained from eq. (2), where $\phi(f)$ is specified from the equation of state. The procedure for the calculation of mean-temperature is not straight forward in the case of clipped-Gaussian distribution. The mathematical details are given in *Appendix 'A'*.

NUMERICAL COMPUTATIONS

The governing equations, eq. (1) are solved numerically using the marching finite difference procedure of Spalding[6]. The computational grid is consisting of 99 cross-stream nodes; and stream-wise step sizes limited to 2% of the current flow width or an entertainment increase of 5% whichever is smaller.

RESULTS AND DISCUSSION

The case study considered for the theoretical investigation is a combusting propane gas jet. Mao *et al.*[1] measured the flow field properties of a combusting propane gaseous flame, stabilised by hydrogen. The exit diameter of the injector was 1.194mm. The test conditions are summarised below:

Propane gas flow rate : 0.176 g/s

Hydrogen gas flow rate : 0.000126 g/s

Initial velocity : 88.7 m/s

Ambient temperature : 300 K

Ambient pressure : 100 kPa

The initial conditions for the numerical computations are prescribed assuming uniform injector properties at the injector exit[1]; therefore, the assumed initial condition is taken to be slug flow, except for a shear layer having a thickness equal to 1% of the jet exit radius at the passage wall. In the uniform flow region, the properties are specified as follows :

$$x = 0,\ r < 0.99\ d/2$$

$$\bar{u}_0 = 4\dot{m}_0/(\rho_0 \pi d^2); \bar{f}_0 = 1$$

$$k_0 = (0.02\,\bar{u}_0)^2;\ \varepsilon_0 = 2.84 \times 10^{-5}\,\bar{u}_0^3/d$$

$$g_0 = 0.$$

The boundary conditions in the region following the potential core of the jet are :

$$r = 0, \frac{\partial \phi}{\partial r} = 0;\ r \to \infty,\ \phi = 0.$$

The quantities $\bar{u}_0$ and $\bar{f}_0$ are assumed to be linear in the shear layer. Initial values of k, ε and g in the shear layer are found by solving their transport equations, while neglecting convection and diffusion terms. The mixture temperature as a function of mixture fraction (state relationship) is calculated based on the thermodynamic principles and shown in Fig. 1. This data has been used to find the mean temperature based on eq. (2). The mean mixture fraction ($\bar{f}$) and square of mixture

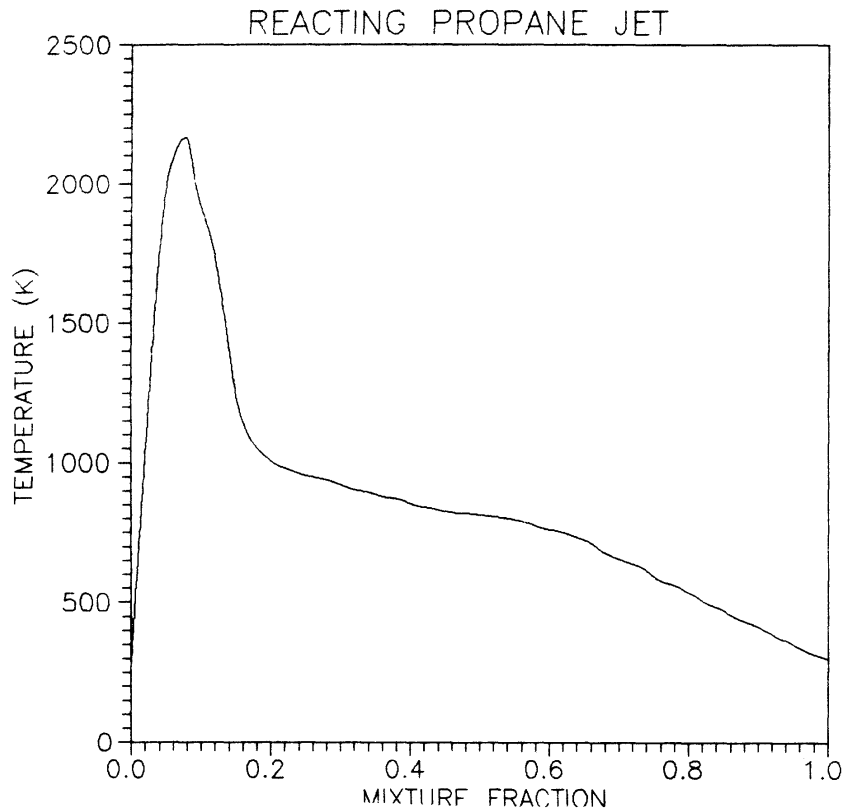

FIG. 1. Variation of temperature with mixture fraction

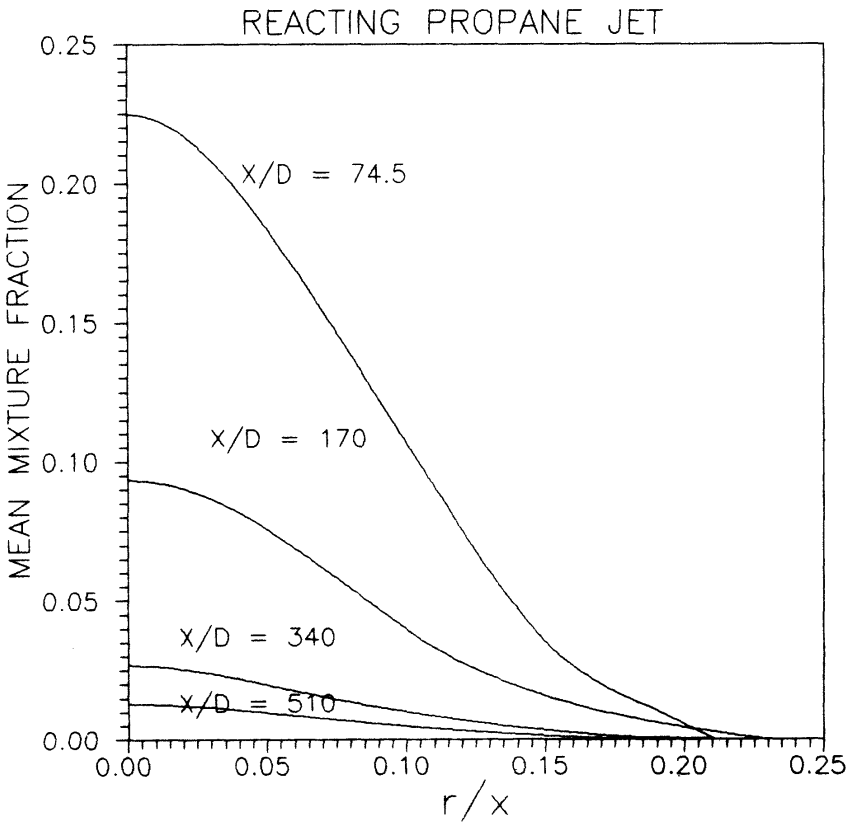

FIG. 2. Radial variation of mean mixture fraction

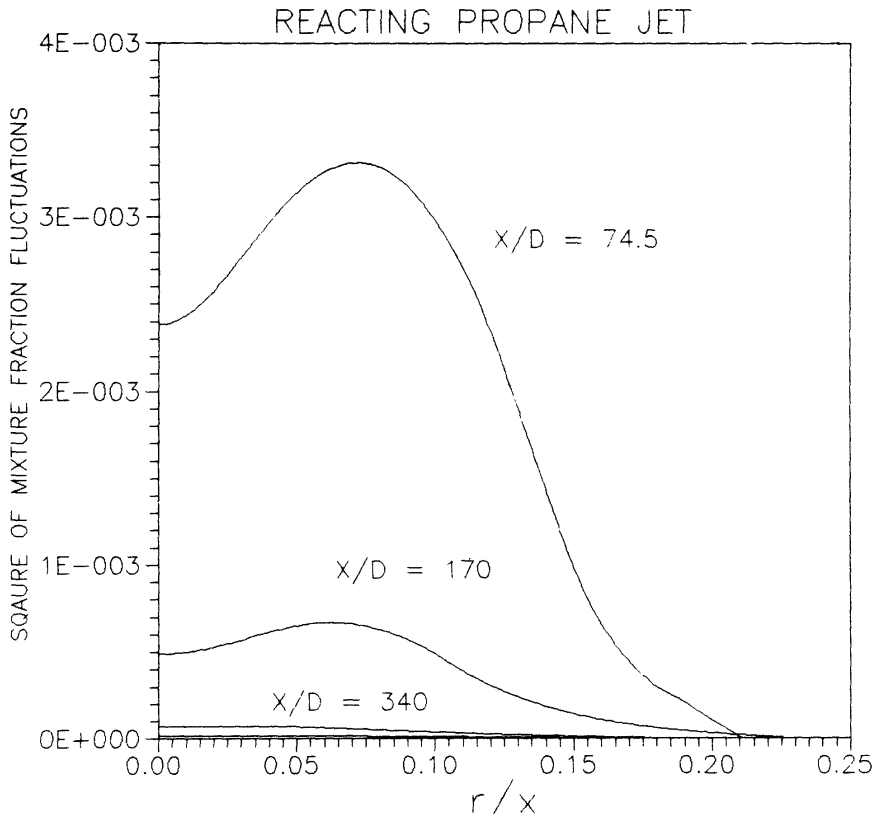

FIG. 3. Radial variation of square of mixture fraction fluctuations

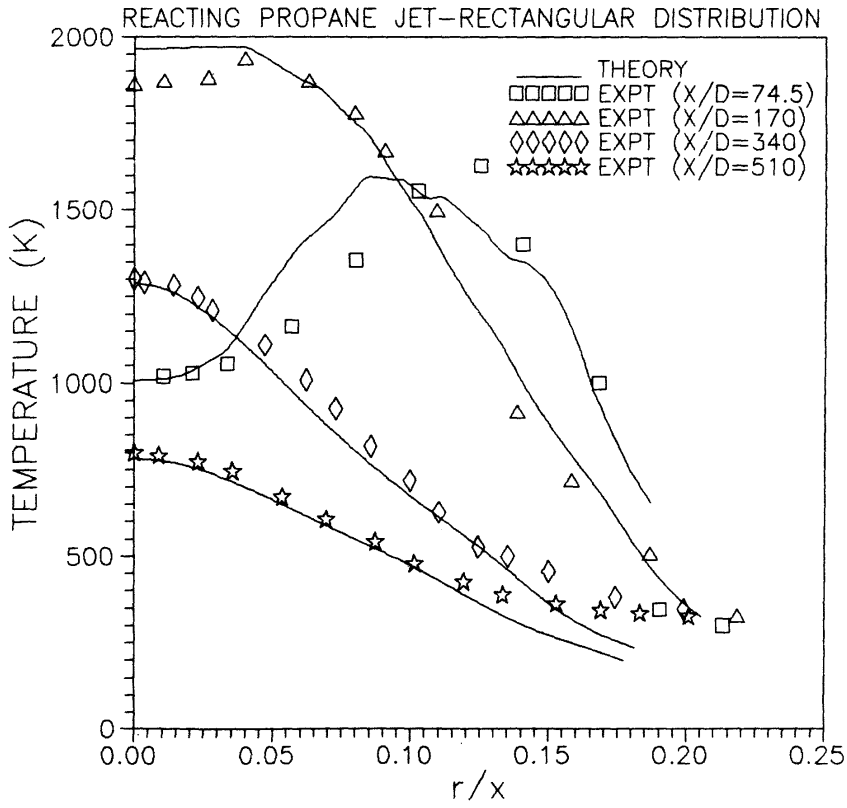

FIG. 4. Radial distribution of temperature

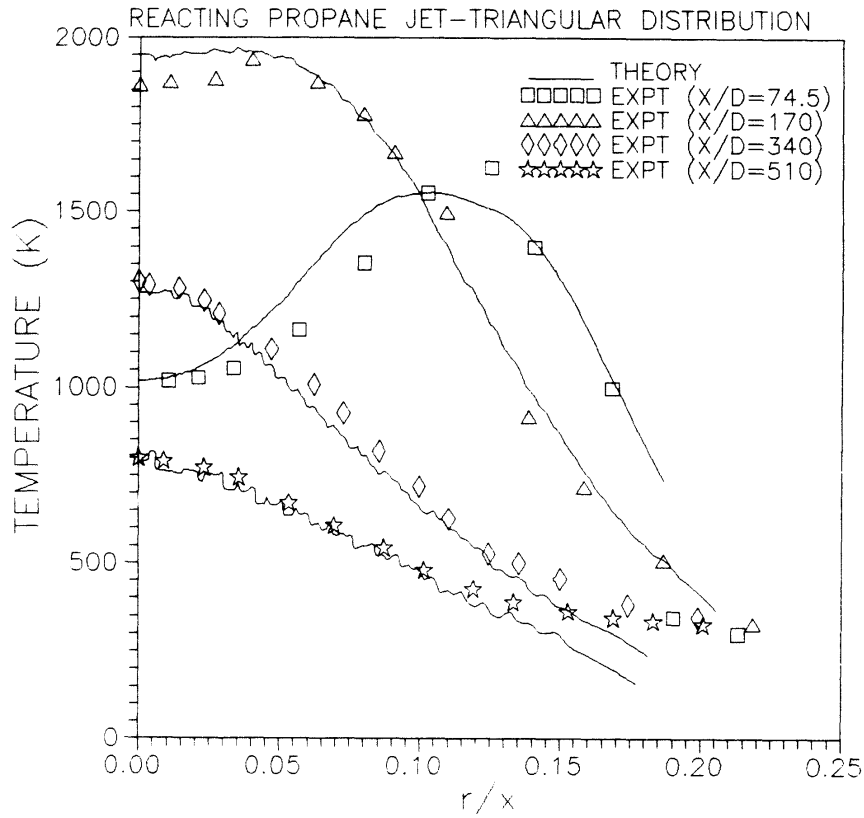

FIG. 5. Radial distribution of temperature

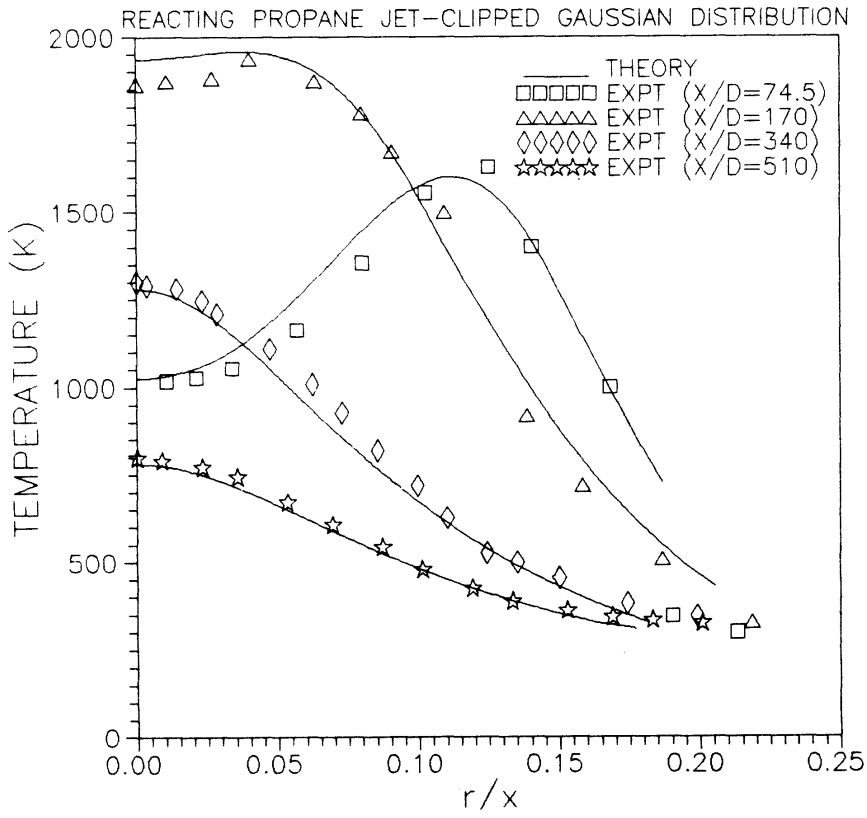

FIG. 6. Radial distribution of temperature

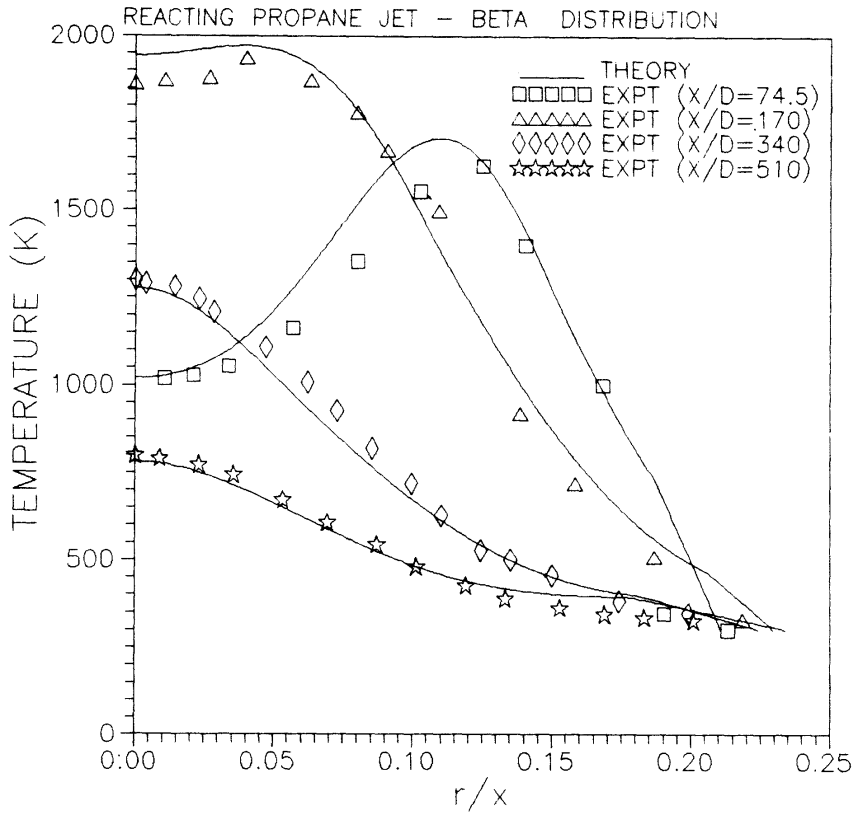

FIG. 7. Radial distribution of temperature

fraction fluctuations (g) are calculated based on eq. (1) in the reactive flow field. The radial distribution of $\tilde{f}$ and g at the axial distances of 74.5, 170, 340 and 510 diameters from the jet exit are shown in Figs. (2) & (3). As the values of g are very low at x/d = 510, it could not be shown in Fig. 3. The maximum values of g at x/d values of 74.5, 170, 340 and 510 are .003153, .000669, .0000736, .000015716 respectively. Figs. (4)-(7) show the radial variation of time averaged mean temperature for various values of x/d such as 74.5, 170, 340 and 510 based on the present computations for the rectangular, triangular, clipped - Gaussian and beta probability density functions respectively. The experimental values of Mao *et al.*[1] are also plotted in the figure.

The agreement between the theory and experiment are close in the near axis regions of the jet flame for all the density functions. At the edge regions the predictions by rectangular and triangular functions are not in agreement with the experimental values. This may be due to very low values of $\tilde{f}$ and g encountered in those regions as shown in Figs. (2) & (3). It is seen from Fig. 5 that the triangular distribution shows a wavy solution which needs some smoothening, if the results are to be used for the design of combustors. The radial distribution of mean temperature based on the clipped-Gaussian distribution and beta distributions predict the values which are in agreement with the experiments of Mao *et al.*[1] throughout the jet flame region as shown in Figs. (6) & (7). Out of the two, the predictions by beta distribution seems to be the best. The predictions show that the maximum mean temperatures are reached away from the axis of the jet. All these temperatures are below the adiabatic flame temperature for stoichiometric combustion (2270 K). These lower values are due to turbulent "unmixedness", which is represented in the calculations by the probability density functions. It is seen that the experimental observations and computations for x/d = 74.5 are providing a different trend compared to that at higher x/d values such as 170, 340 &

510. This implies that the flow at x/d = 74.5 is a developing flow (potential and transition to fully developed state) and at $x/d \geq 170$ the flow is developed. The locations of uncertainty have been identified as the regions near nozzle exit ($x/d \leq 74.5$) and close to the jet edges ($r/x > 0.1$). If the validation is reasonable in those regions, then the performance of that particular model can be assumed to be the best. As the validation in those regions are reasonably close (Fig. 7), the beta distribution has been termed the best suited for the prediction of turbulent jet flame.

CONCLUSIONS

The following conclusions have been arrived at based on the numerical study carried out on non-premixed turbulent jet flame :

1. The flow field modeling was based on the locally homogeneous flow model.

2. In order to calculate the turbulent "unmixedness" in the flow field of a turbulent jet flame, various probability density functions such as rectangular, triangular, clipped-Gaussian and beta distributions have been used and the mean mixture temperatures in the flow field are computed.

3. The rectangular and triangular distributions fail to predict correctly the mean temperatures near the edges of the jet flame.

4. The clipped-Gaussian and beta distributions predict the whole flow field in close agreement with the experimental values reported in literature.

TABLE I : Source terms in equation (1)

$\bar{\phi}$	$\mu_{eff,\phi}$	S_ϕ
1	-	0
$\bar{u}$	$\mu + \mu_t$	$a(\rho_\infty - \bar{\rho})$
$\bar{f}$	$(\mu/SC) + (\mu_t/\sigma_f)$	0
k	$\mu + (\mu_t/\sigma_k)$	$\mu_t (\partial \bar{u}/\partial r)^2 - \bar{\rho}\,\varepsilon$
ε	$\mu + (\mu_t/\sigma_\varepsilon)$	$\{C_{\varepsilon_1} \mu_t (\partial \bar{u}/\partial r)^2 - C_{\varepsilon_2} \bar{\rho}\,\varepsilon\}\ (\varepsilon/k)$
g	$\mu/SC + \mu_t/\sigma_g$	$C_{g_1} \mu_t (\partial \bar{f}/\partial r)^2 - C_{g_2} \bar{\rho}\, g\, \varepsilon/k$

C_μ = 0.09; $C_{\varepsilon 1}$ = 1.44; $C_{\varepsilon 2}$ = 1.87; C_{g_1} = 2.7; C_{g_2} = 1.79; σ_k = 1.0; $\sigma_f = \sigma_g$ = 0.7; SC = 0.7.

ACKNOWLEDGEMENT

The authors thank Professor G. S. Mani, Director & Dean, Institute of Armament Technology, Pune, for his encouragement to publish this work and Dr M. Ganapathi and Dr S. E. Talole for their help in mathematical derivations.

REFERENCES

1. C. P. Mao, G. A. Szekely and G. M. Faeth, Evaluation of a Locally Homogeneous Flow Model of Spray Combustion, NASA CR-3202, 1980.
2. A. J. Shearer, H. Tamura and G. M. Faeth, *J. Energy*, **3** (1979) 271-75.
3. V. Ramanujachari and R. Natarajan, *XII NCICEC, Dehradun* (1992) 547-52.

4. S. Ganesan and V. Ramanujachari, *XV NCICEC, Chennai* (1997) 562-66.
5. S. Ganesan, S. Balakrishna and V. Ramanujachari, *Indian J. pure appl. Math.* **30** (1999) 167-73.
6. D. B. Spalding, *GENMIX : A General Computer Program for Two-Dimensional Parabolic Phenomena*, Pergamon Press, 1977.

APPENDIX 'A'

Clipped-Gaussian Distribution

The Gaussian distribution is given by:

$$P_1(f) = \frac{1}{\sigma\sqrt{2\pi}} e^{-1/2\left(\frac{f-\mu}{\sigma}\right)^2}, \quad \ldots (1)$$

where μ is the mean value of the mixture fraction f and σ is the standard deviation.

The equation for clipped-Gaussian distribution clipped at $f = 0$ and $f = 1$ is of the form :

$$P(f) = \frac{1}{\sigma\sqrt{2\pi}} e^{-1/2\left(\frac{f-\mu}{\sigma}\right)^2} [H(f) - H(f-1)] + A\,\delta(0) + B\delta(1), \quad \ldots (2)$$

where $H(f)$ and $\delta(f)$ are Heaviside step function and Dirac delta function respectively. The values of A and B are obtainable by integrating eq. (1), where :

$$A = \int_{-\infty}^{0} P_1(f)\,df \text{ and } B = \int_{1}^{\infty} P_1(f)df.$$

The dimensions of the clipped-Gaussian distribution are found from the mean $\bar{f}$, and the variance, g. Taking the first and second moments about $f = 0$ and $f = \bar{f}$ respectively, we obtain:

$$\bar{f} = \int_{-\infty}^{\infty} f P(f)\,df \quad \ldots (3)$$

and

$$g = \int_{-\infty}^{\infty} f^2 P(f)\,df - \bar{f}^2. \quad \ldots (4)$$

Eqs. (3) and (4) are integrated by the substitution of $P(f)$ from eq. (2). The following expressions are obtained for $\bar{f}$ and g.

$$\bar{f} = 1 + (\mu - 1)\,P(z_1) - \mu\,P(z_0) + \frac{\sigma}{\sqrt{2\pi}}\left[e^{-Z_0^2/2} - e^{-Z_1^2/2} \right], \quad \ldots (5)$$

where,

$$P(z) = \frac{1}{\sqrt{2\pi}} \int_{-\infty}^{z} e^{-1/2Z^2}\,dz$$

or,

$$P(z) = \frac{1}{2} + \frac{1}{2} erf\left(\frac{z}{\sqrt{2}} \right),\ P(z_1) = \frac{1}{2} + \frac{1}{2} erf\left(\frac{1-\mu}{\sigma\sqrt{2}} \right),\ P(z_0) = \frac{1}{2} + \frac{1}{2} erf\left(\frac{-\mu}{\sigma\sqrt{2}} \right)$$

where

$$erf(x) = \frac{2}{\sqrt{\pi}} \int_0^x e^{-w^2}\, dw$$

$$z_1 = \frac{1-\mu}{\sigma},\ z_0 = \frac{-\mu}{\sigma},\ z = \frac{\bar{f}-\mu}{\sigma}$$

and

$$g = 1 + (\sigma^2 + \mu^2 - 1)\, P(z_1) - (\sigma^2 + \mu^2)\, P(z_0) + \frac{\sigma^2}{\sqrt{2\pi}} \left(z_0\, e^{-z_0^2/2} - z_1\, e^{-z_1^2/2} \right)$$

$$+ \frac{2\sigma\mu}{\sqrt{2\pi}} \left(e^{-z_0^2/2} - e^{-z_1^2/2} \right) - \bar{f}^2. \qquad \ldots (6)$$

Rewriting eqs. (5) & (6) gives :

$$F(\mu, \sigma) = \{\text{RHS of Eq. (5)}\} - \bar{f} = 0, \qquad \ldots (7)$$

$$G(\mu, \sigma) = \{\text{RHS of Eq. (6)}\} - g = 0, \qquad \ldots (8)$$

$$\frac{\partial F}{\partial \mu} = (\mu - 1) \frac{\partial P(z_1)}{\partial \mu} + P(z_1) - \mu \frac{\partial P(z_0)}{\partial \mu}$$

$$- P(z_0) - \frac{1}{\sigma\sqrt{2\pi}} \left[\mu\, e^{-z_0^2/2} + (1-\mu)\, e^{-z_1^2/2} \right], \qquad \ldots (9)$$

$$\frac{\partial F}{\partial \sigma} = (\mu - 1) \frac{\partial P(z_1)}{\partial \sigma} - \mu \frac{\partial P(z_0)}{\partial \sigma} + \frac{1}{\sigma^2\sqrt{2\pi}} \left[\mu^2\, e^{-\frac{z_0^2}{2}/2} + (1-\mu)\, e^{-z_1^2/2} \right]$$

$$+ \frac{1}{\sqrt{2\pi}} \left[e^{-\frac{z_0^2}{2}/2} + e^{-z_1^2/2} \right], \qquad \ldots (10)$$

$$\frac{\partial G}{\partial \mu} = (\sigma^2 + \mu^2 - 1) \frac{\partial P(z_1)}{\partial \mu} + 2\mu\, P(z_1) - (\sigma^2 + \mu^2) \frac{\partial P(z_0)}{\partial \mu} - 2\mu\, P(z_0) + \frac{\sigma}{\sqrt{2\pi}}$$

$$\left[\frac{\mu^2}{\sigma^2} e^{-\frac{z_0^2}{2}/2} + e^{-\frac{z_0^2}{2}/2} - \frac{(1-\mu)^2}{\sigma^2} e^{-\frac{z_1^2}{2}/2} + e^{-\frac{z_1^2}{2}/2} \right] - \qquad \ldots (11)$$

$$\frac{2\mu}{\sigma\sqrt{2\pi}} \left[\mu\, e^{-\frac{z_0^2}{2}} + (1-\mu)\, e^{-z_1^2/2} \right] + \frac{2\sigma}{\sqrt{2\pi}} \left[e^{-\frac{z_1^2}{2}/2} + e^{-\frac{z_1^2}{2}/2} \right]$$

and

$$\frac{\partial G}{\partial \sigma} = (\sigma^2 + \mu^2 - 1)\frac{\partial P(z_1)}{\partial \sigma} + 2\sigma P(z_1) - (\sigma^2 + \mu^2)\frac{\partial P(z_0)}{\partial \sigma} - 2\sigma P(z_0) + \frac{1}{\sqrt{2\pi}}$$

$$\left[\frac{\mu^3}{\sigma^2} e^{\frac{-z_0^2}{2}} + \mu e^{-z_0^2/2} - \frac{(1-\mu)^3}{\sigma^2} e^{-\frac{z_1^2}{2}} + (1-\mu) e^{-z_1^2/2} \right] +$$

$$\frac{2\sigma}{\sigma\sqrt{2\pi}}\left[Z_0 e^{-\frac{z_0^2}{2}} + z_1 e^{-z_1^2/2} \right] + \frac{2\mu}{\sqrt{2\pi}}\left[e^{-\frac{z_0^2}{2}} + e^{-z_1^2/2} \right]$$

$$+ \frac{2\mu}{\sigma^2\sqrt{2\pi}}\left[\mu^2 e^{-\frac{z_0^2}{2}} - (1-\mu)^2 e^{-z_1^2/2} \right],$$

where

$$\frac{\partial P(z_1)}{\partial \mu} = -\frac{1}{\sigma\sqrt{2\pi}} e^{\frac{-z_1^2}{2}}, \quad \frac{\partial P(z_1)}{\partial \sigma} = -\frac{1-\mu}{\sigma^2\sqrt{2\pi}} e^{-\frac{z_1^2}{2}}, \quad \frac{\partial P(z_0)}{\partial \mu} = -\frac{1}{\sigma\sqrt{2\pi}} e^{-\frac{z_0^2}{2}}$$

and

$$\frac{\partial P(z_0)}{\partial \sigma} = \frac{\mu}{\sigma^2\sqrt{2\pi}} e^{-\frac{z_0^2}{2}}.$$

From eqs. (7)-(12) solution can be obtained as follows :

$$\begin{bmatrix} \mu_1 \\ \sigma_1 \end{bmatrix} = \begin{bmatrix} \mu_0 \\ \sigma_0 \end{bmatrix} - \begin{bmatrix} \frac{\partial F}{\partial \mu} & \frac{\partial F}{\partial \sigma} \\ \frac{\partial G}{\partial \mu} & \frac{\partial G}{\partial \sigma} \end{bmatrix}^{-1} \begin{bmatrix} F(\mu_0, \sigma_0) \\ G(\mu_0, \sigma_0) \end{bmatrix}$$

The final solution depends on the initial guess values μ_0 & σ_0. The initial guess values assigned in the present work are $\mu_0 = \bar{f}$ and $\sigma_0 = \sqrt{g}$. The values of $\bar{f}$ and g are known in the flow field.